

## Electronic Supplementary Information

### **Dy<sub>2</sub>NiRuO<sub>6</sub> perovskite with high activity and durability for the oxygen evolution reaction in acidic electrolyte**

Isabel Rodríguez-García <sup>a</sup>, José Luis Gómez de la Fuente <sup>a</sup>, Dmitry Galyamin <sup>a</sup>, Álvaro Tolosana-Moranchel <sup>a</sup>, Paula Kayser <sup>b,c</sup>, Mohamed Abdel Salam <sup>d</sup>, José Antonio Alonso <sup>b</sup>, Federico Calle-Vallejo, <sup>e,f</sup> Sergio Rojas <sup>a\*</sup>, María Retuerto <sup>a\*</sup>

<sup>a</sup> Grupo de Energía y Química Sostenibles, Instituto de Catálisis y Petroleoquímica, CSIC, C/Marie Curie 2, 28049, Madrid, Spain

<sup>b</sup> Instituto de Ciencia de Materiales de Madrid, CSIC., C/Sor Juana Inés de la Cruz 3, 28049 Madrid, Spain

<sup>c</sup> Dep. Q. Inorgánica I, Fa Químicas, Universidad Complutense, Avda. Complutense s/n, 28040-Ciudad Universitaria, Madrid, Spain

<sup>d</sup> Chemistry Department, Faculty of Science, King Abdulaziz University, P. O Box 80200, Jeddah, 21589, Saudi Arabia

<sup>e</sup> Nano-Bio Spectroscopy Group and European Theoretical Spectroscopy Facility (ETSF), Department of Advanced Materials and Polymers: Physics, Chemistry and Technology, University of the Basque Country UPV/EHU, Avenida Tolosa 72, 20018 San Sebastián, Spain.

<sup>f</sup> IKERBASQUE, Basque Foundation for Science, Plaza de Euskadi 5, 48009 Bilbao, Spain.

### Table of Contents

<b>S1. Crystal structure of R<sub>2</sub>NiRuO<sub>6</sub>.....</b>	<b>2</b>
<b>S2. Additional electrochemical results.....</b>	<b>4</b>
<b>S3. TEM characterization.....</b>	<b>12</b>
<b>S4. XPS results of the initial and cycled Dy<sub>2</sub>NiRuO<sub>6</sub> catalyst.....</b>	<b>13</b>
<b>S5. Full computational details.....</b>	<b>14</b>
<b>S6. Additional references.....</b>	<b>21</b>

## S1. Crystal structure of $R_2NiRuO_6$

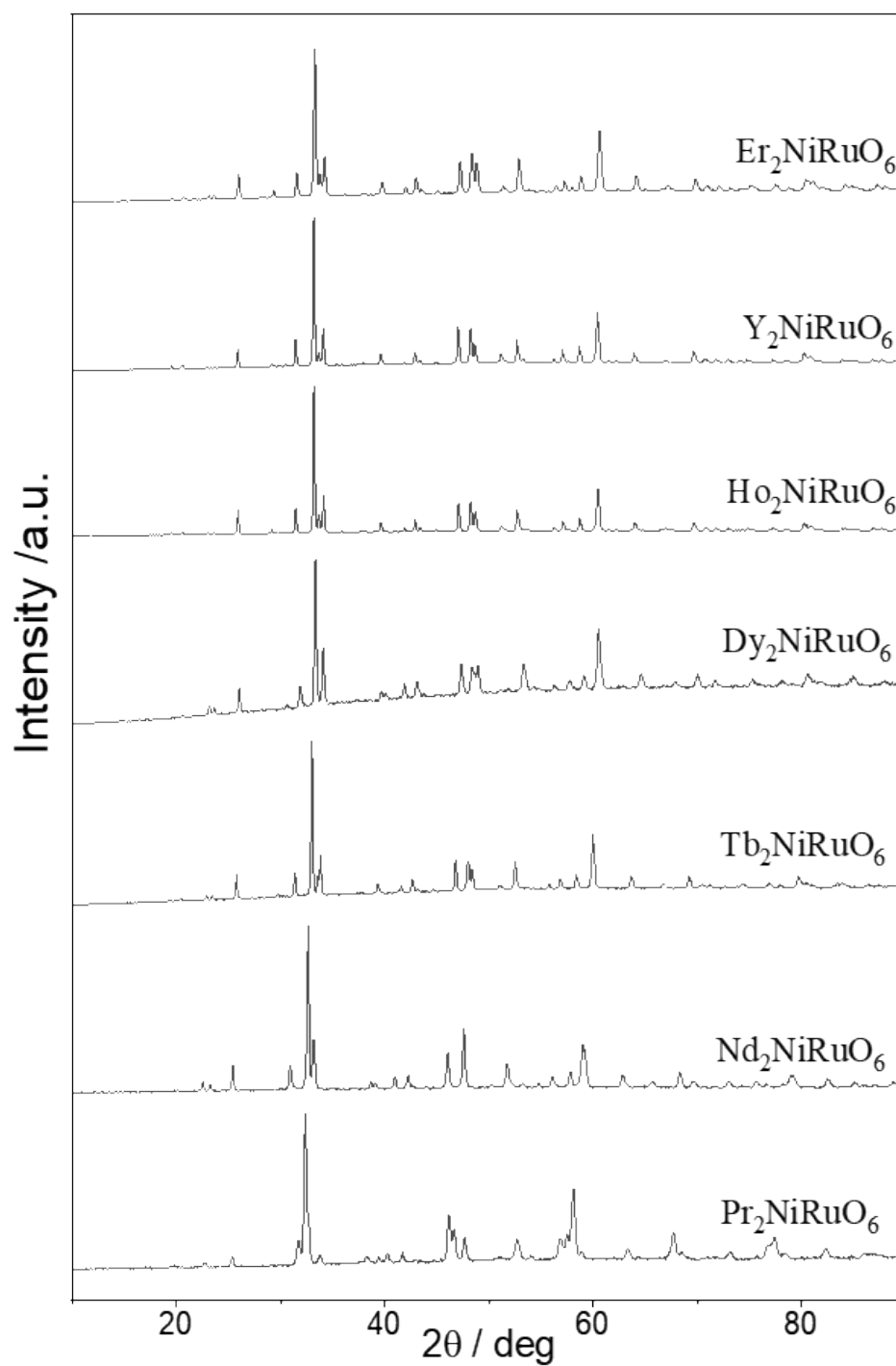


**Figure S1.** X-ray diffractograms for as prepared  $R_2NiRuO_6$  initial catalysts.

**Table S1.** Cell parameters and volume for  $R_2NiRuO_6$  from XRD Rietveld refinements.

<b>Oxide</b>	<b>Cell Parameters (Å)</b>	<b>Volume (Å<sup>3</sup>)</b>
<i>Dy<sub>2</sub>NiRuO<sub>6</sub></i>	a = 5.27718(8) b = 5.6931(1) c = 7.5671(1)	227.343(6)
	β = 89.963(3)	
<i>Er<sub>2</sub>NiRuO<sub>6</sub></i>	a = 5.2412(3) b = 5.6718(3) c = 7.5349(4)	223.991(2)
	β = 90.097(6)	
<i>Ho<sub>2</sub>NiRuO<sub>6</sub></i>	a = 5.2560(2) b = 5.6872(2) c = 7.5475(3)	225.67(1)
	β = 89.931(5)	
<i>Nd<sub>2</sub>NiRuO<sub>6</sub></i>	a = 5.3929(3) b = 5.7826(3) c = 7.6483(5)	238.51(3)
	β = 90.080(9)	
<i>Pr<sub>2</sub>NiRuO<sub>6</sub></i>	a = 5.4841(5) b = 5.6462(5) c = 7.7867(7)	241.11(4)
	β = 89.91(1)	
<i>Tb<sub>2</sub>NiRuO<sub>6</sub></i>	a = 5.2992(2) b = 5.7047(2) c = 7.5906(3)	229.47(2)
	β = 90.070(5)	
<i>Y<sub>2</sub>NiRuO<sub>6</sub></i>	a = 5.2577(2) b = 5.6876(2) c = 7.5457(2)	225.61(1)
	β = 89.921(4)	

## S2. Additional electrochemical results

**Table S2.** Ru-containing oxides (without Ir) reported as electrocatalysts for the OER in acid. The current densities shown are the highest values reported. The values are reported for the initial cycle, after 10 cycles (\*) or after 30 cycles (\*\*).

Catalyst	E-iR / V @ 10 mA·cm <sup>-2</sup>	Tafel slope / mV dec <sup>-1</sup>	Durability test
<b>Perovskites</b>			
Dy <sub>2</sub> NiRuO <sub>6</sub> (this work)	1.507**	55.8	500 cycles (1.1-1.7 V @ 10 mV s <sup>-1</sup> ) decrease 35% activity.
Er <sub>2</sub> NiRuO <sub>6</sub> (this work)	1.624**	~170	60 cycles (1.1-1.7 V @ 10 mV s <sup>-1</sup> ) decrease 28% activity
Ho <sub>2</sub> NiRuO <sub>6</sub> (this work)	1.647	~138	30 cycles (1.1-1.7 V @ 10 mV s <sup>-1</sup> ) decrease 26% activity
Tb <sub>2</sub> NiRuO <sub>6</sub> (this work)	1.591	~128	30 cycles (1.1-1.7 V @ 10 mV s <sup>-1</sup> ) decrease 46% activity
Y <sub>2</sub> NiRuO <sub>6</sub> (this work)	1.604**	~159	500 cycles (1.1-1.7 V @ 10 mV s <sup>-1</sup> ) decrease 97% activity
Sr <sub>1-x</sub> Na <sub>x</sub> RuO <sub>3</sub> <sup>1</sup>	1.39	40	20 cycles (1.1-1.5 V @ 10 mV s <sup>-1</sup> ) decrease 15% activity
Sr <sub>1-x</sub> K <sub>x</sub> RuO <sub>3</sub> <sup>2</sup>	1.38	59	20 cycles (1.1-1.5 V @ 10 mV s <sup>-1</sup> ) decrease 25% activity
SrRuO <sub>3</sub> <sup>3</sup>		51.5	Loss of activity after first cycle
CaCu <sub>3</sub> Ru <sub>4</sub> O <sub>12</sub> <sup>4</sup>	1.401	40	Stable 24 h @ 10 mAcm <sup>-2</sup>
<b>Pyrochlores</b>			
Y <sub>2</sub> RuMnO <sub>7</sub> <sup>5</sup>	1.49	48	Stable 45 h @ 10 mAcm <sup>-2</sup>
Dy <sub>2</sub> RuMnO <sub>7</sub> <sup>5</sup>	1.51	47	Stable 25 h @ 10 mAcm <sup>-2</sup>
Tb <sub>2</sub> RuMnO <sub>7</sub> <sup>5</sup>	1.54	56	Stable 15 h @ 10 mAcm <sup>-2</sup>
Y <sub>1.7</sub> Sr <sub>0.3</sub> Ru <sub>2</sub> O <sub>7</sub> <sup>6</sup>	1.494	44.8	-
Y <sub>1.85</sub> Zn <sub>0.15</sub> Ru <sub>2</sub> O <sub>7-δ</sub> <sup>7</sup>	1.521	36.9	-
Y <sub>2</sub> [Ru <sub>1.6</sub> Y <sub>0.4</sub> ]O <sub>7-δ</sub> <sup>8</sup>	1.48	37	-
Y <sub>1.8</sub> Fe <sub>0.2</sub> Ru <sub>2</sub> O <sub>7-δ</sub> <sup>9</sup>	1.625*	52-63	-
Y <sub>1.8</sub> Cu <sub>0.2</sub> Ru <sub>2</sub> O <sub>7-δ</sub> <sup>9</sup>	1.58*	52-63	Stable 6 h @ 1 mA cm <sup>-2</sup> <sub>geo</sub>
Y <sub>1.8</sub> Ni <sub>0.2</sub> Ru <sub>2</sub> O <sub>7-δ</sub> <sup>9</sup>		52-63	-
Y <sub>1.8</sub> Co <sub>0.2</sub> Ru <sub>2</sub> O <sub>7-δ</sub> <sup>9</sup>		52-63	-
Y <sub>2x</sub> Ba <sub>x</sub> Ru <sub>2</sub> O <sub>7-δ</sub> <sup>10</sup>	1.508	40.8	1500 cycles bt. 1.4-1.6 V
Y <sub>2</sub> Ru <sub>2</sub> O <sub>7</sub> <sup>11</sup>	1.561(5) *	40	Stable 1 h @ 1.56 V

$\text{Nd}_2\text{Ru}_2\text{O}_7$ <sup>11</sup>	1.576(9)*	41	Stable 1 h @ 1.56 V
$\text{Gd}_2\text{Ru}_2\text{O}_7$ <sup>11</sup>	1.590(7)	47	Stable 1 h @ 1.56 V
$\text{Bi}_2\text{Ru}_2\text{O}_7$ <sup>11</sup>	1.588(7) *	48	Stable 1 h @ 1.56 V
$\text{Y}_2\text{Ru}_2\text{O}_{7-\delta}$ <sup>12</sup>	1.55	55	Almost stable after 10000 cycles (1.35-1.6 V @ 100 mV s <sup>-1</sup> )
<b>Ru and Ru-based Simple Oxides</b>			
$\text{Cr}_{0.6}\text{Ru}_{0.4}\text{O}_2$ <sup>13</sup>	1.405	58	10 h @ 10 mAc <sup>m-2</sup>
$\text{W}_{0.2}\text{Er}_{0.1}\text{Ru}_{0.7}\text{O}_{2-\delta}$ <sup>14</sup>	1.43	66.8	500 h @ 10 mAc <sup>m-2</sup>
$\text{Ru-MnO}_2$ <sup>15</sup>	1.391	29.4	Almost stable 200 h @ 10mAc <sup>m-2</sup>
Cu-doped $\text{RuO}_2$ <sup>16</sup>	1.418	43.96	Stable 8 h @ 10mAc <sup>m-2</sup>
Co-doped $\text{RuO}_2$ <sup>17</sup>	1.43		-
Co- $\text{RuO}_2$ /Ni- $\text{RuO}_2$ <sup>17</sup>	1.537	58.2	-
$\text{RuO}_2$ <sup>11</sup>	1.626(14)*	77	Stable 1 h @ 1.56 V
$\text{RuO}_2$ NSs <sup>18</sup>	1.429		6 h @ 1 mA cm <sup>-2</sup> to 10 mA cm <sup>-2</sup>
$\text{Ru-Pt}_3\text{Cu}$ <sup>19</sup>	1.45		Almost stable 28 h @ 10 mA cm <sup>-2</sup>

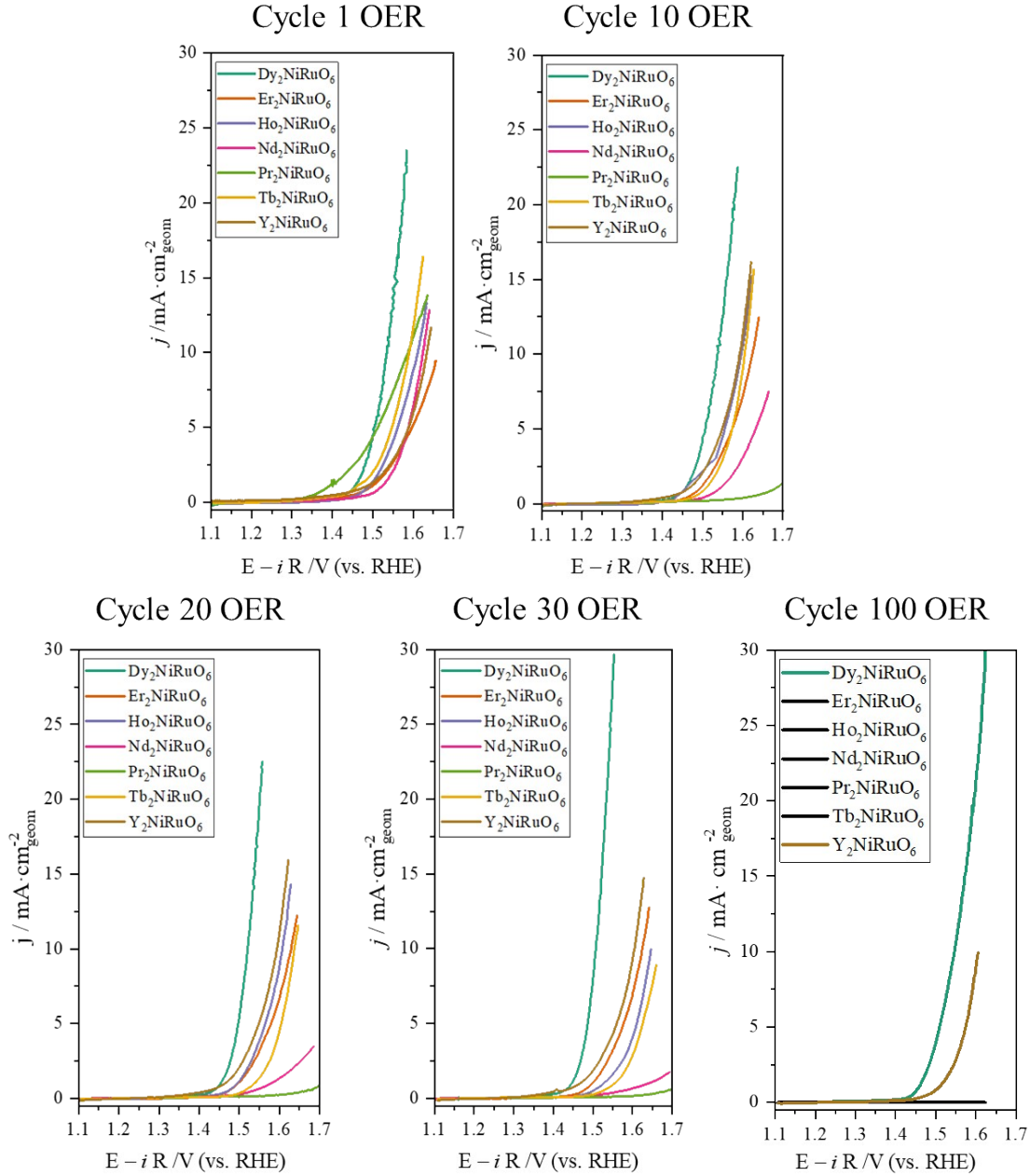


**Figure S2.** Evolution of the OER activity of  $R_2NiRuO_6$ , measured in  $O_2$ -saturated 0.1 M  $HClO_4$  at 1600 rpm.

Figure S3 shows the Nyquist plot of the values obtained at 1.5 V vs RHE of the initial  $Dy_2NiRuO_6$  and after 50 cycles. We notice the presence of a single semicircle corresponding to a typical equivalent circuit of a solution resistance ( $R_s$ ) in series to  $R_{ct}$  in parallel to  $CPE_{dl}$ . As expected from the CVs in Figure 2 and Figure S2, in which the activity increases after the first few cycles,  $R_{ct}$  decreases proportionally.

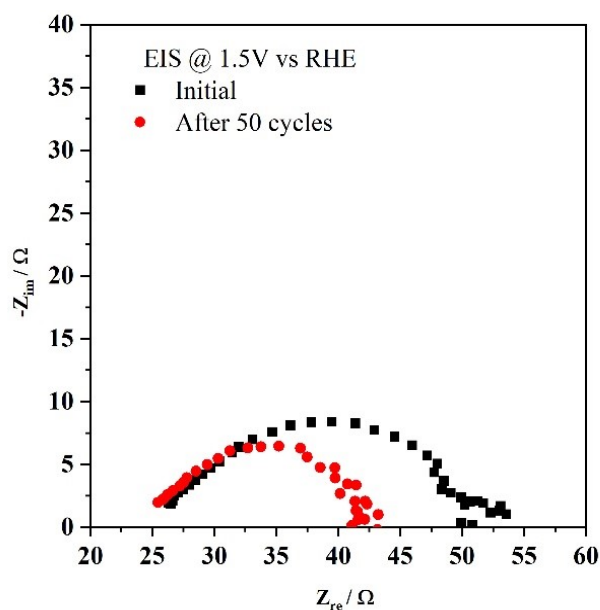
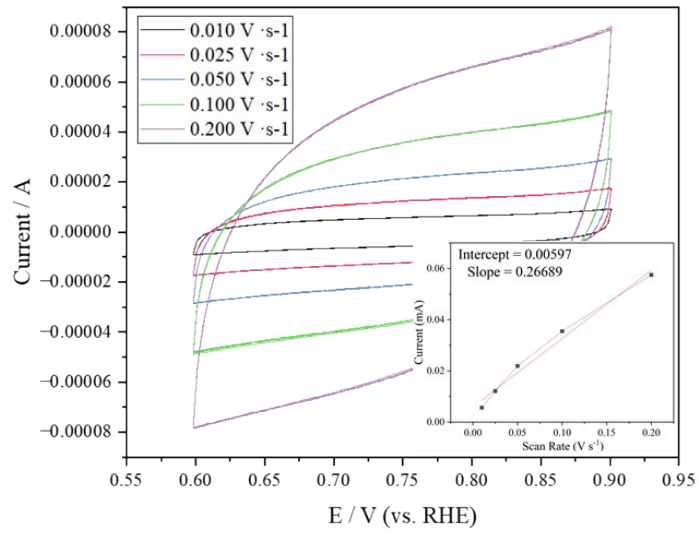


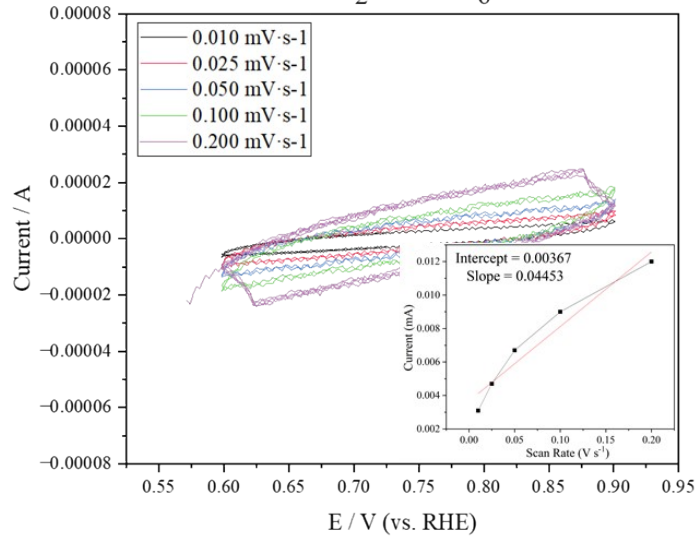
**Figure S3.** Nyquist plot of the measurements obtained at 1.5 V vs RHE of the initial (black)  $\text{Dy}_2\text{NiRuO}_6$  and after 50 OER cycles (red).

The electrochemically active surface area (ECSA) was calculated by the double-layer capacitance ( $C_{\text{dl}}$ ) of each catalyst. We performed CVs close to the “open circuit potential” in argon-saturated electrolyte (Figure S4) to ensure that the currents obtained are due only to the double-layer capacitance. The cyclic voltammograms are performed at multiple scan rates and the double-layer charging current is equal to the product of the scan rate ( $\nu$ ) and the  $C_{\text{dl}}$  as shown in the following equation:  $i_c = \nu C_{\text{dl}}$ . Plotting  $i_c$  as a function of  $\nu$ , the slope is the capacitance  $C_{\text{dl}}$ , and then  $\text{ECSA} = C_{\text{dl}} / C_s$ , where  $C_s$  is the specific capacitance of an atomically flat planar surface of the material per unit area under identical electrolyte conditions. As value of  $C_s$  for oxides is ill-defined, we use  $0.06 \text{ mF/cm}^2$ , in line with previous references.<sup>20,21</sup>

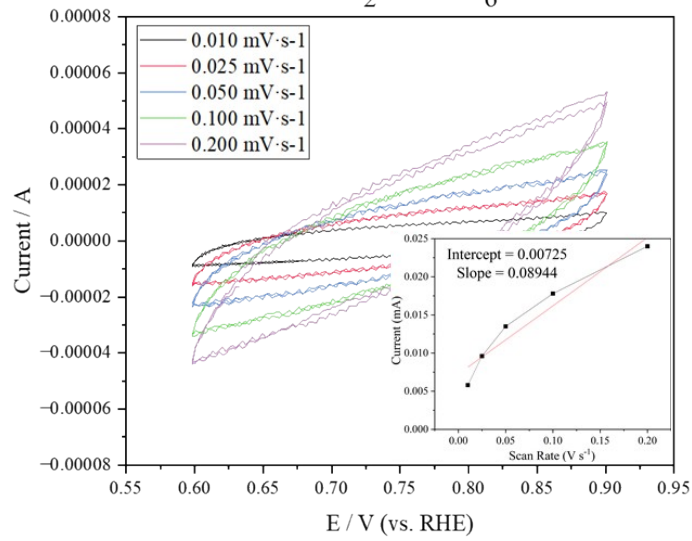
### Dy<sub>2</sub>NiRuO<sub>6</sub>



### Er<sub>2</sub>NiRuO<sub>6</sub>

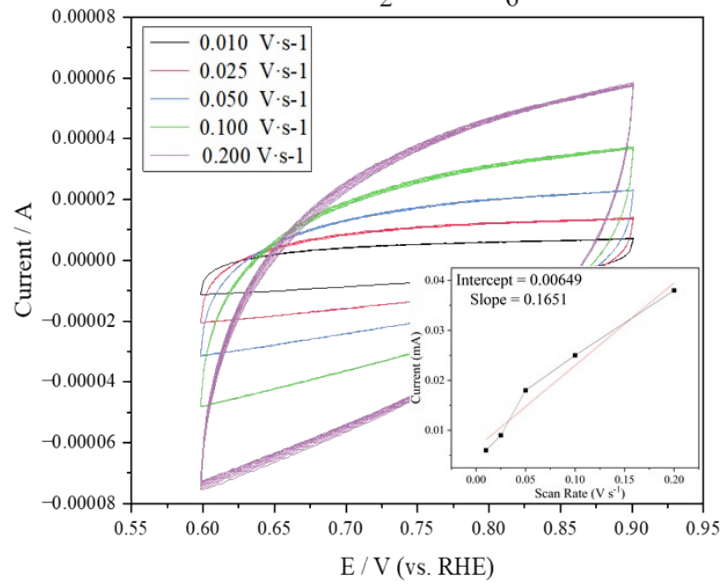


### Ho<sub>2</sub>NiRuO<sub>6</sub>

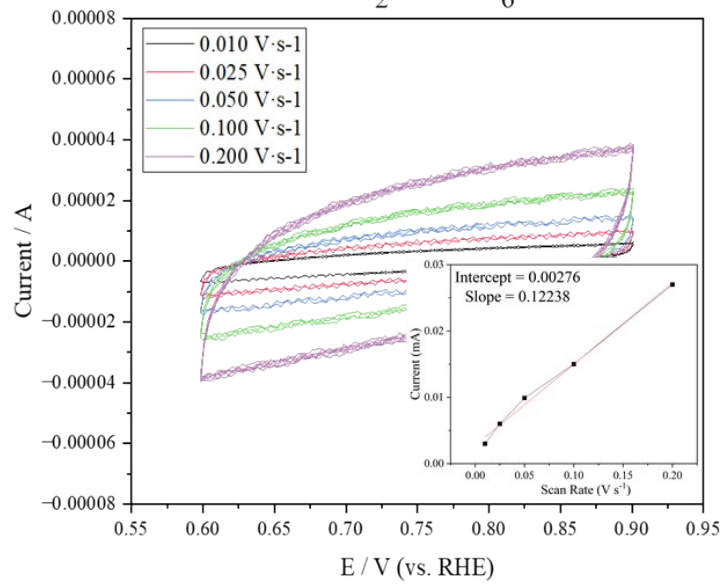




### Nd<sub>2</sub>NiRuO<sub>6</sub>



### Tb<sub>2</sub>NiRuO<sub>6</sub>



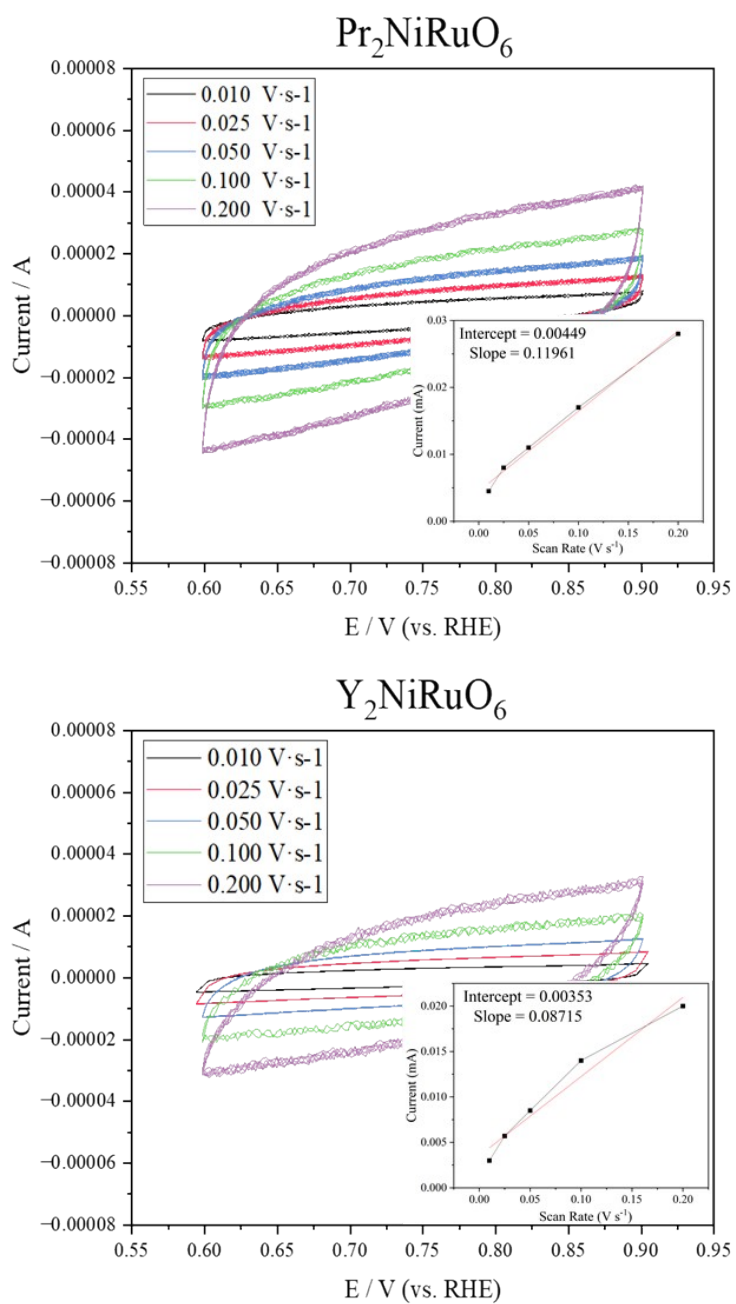


**Figure S4.** CVs measured at multiple scan rates close to the “open circuit potential” in argon-saturated 0.1 M  $\text{HClO}_4$  electrolyte for  $\text{R}_2\text{NiRuO}_6$  samples. Inset: currents obtained at a certain potential vs. scan rate and the corresponding linear fits.

**Table S3.** ECSA for R<sub>2</sub>NiRuO<sub>6</sub>.

<b>R<sub>2</sub>NiRuO<sub>6</sub></b>	<b>ECSA (m<sup>2</sup> g<sup>-1</sup>)</b>
<i>R = Dy</i>	8.8
<i>R = Er</i>	1.4
<i>R = Ho</i>	3.0
<i>R = Nd</i>	5.4
<i>R = Pr</i>	4.0
<i>R = Tb</i>	4.0
<i>R = Y</i>	3.0

C<sub>dl</sub> can be determined either by CV or by electrochemical impedance spectroscopy (EIS). Nevertheless, when measuring C<sub>dl</sub> by EIS, it is possible to obtain more information by replacing C<sub>dl</sub> with a constant phase element (CPE<sub>dl</sub>).

The CPE expression is  $Z_{CPE} = \frac{1}{(j\omega)^\varphi T_{dl}}$ , where *j* is the imaginary unit,  $\omega$  is the angular frequency,  $\varphi$  is the dimensionless exponent that represents the (non)ideality of the capacitance and T<sub>dl</sub> is a double-layer capacitance related parameter. As T<sub>dl</sub> is in units of F s $\varphi^{-1}$ , it is not directly proportional to the electrode surface area. To know

the exact value of C<sub>dl</sub>, in F, the following equation is used  $C_{dl} = T_{dl}^\varphi \left(\frac{1}{R_s}\right)^{1-\frac{1}{\varphi}}$ . Additionally, if C<sub>dl</sub> is measured at a potential in which the OER occurs, information on the kinetics of the reaction can also be obtained since the value of the charge transfer resistance (R<sub>ct</sub>) can be determined.<sup>22</sup>

To better study the surface changes, ECSA<sub>EIS</sub> calculated from the T<sub>dl</sub> has been represented as a function of the cycles for Dy<sub>2</sub>NiRuO<sub>6</sub> (Figure S5). During the first 150 cycles, ECSA<sub>EIS</sub> decreases from approximately 17 to 13 m<sup>2</sup> g<sup>-1</sup>, and the latter value is maintained during the following cycles. Analogously,  $\varphi$  increases during the first cycles from approximately 0.82 to 0.87, indicating a more homogeneous surface. Note that the ECSA value obtained by EIS is higher, yet in the same order of magnitude, than that obtained by scan-rate dependent CVs. This feature has been previously observed by other authors.<sup>20</sup>

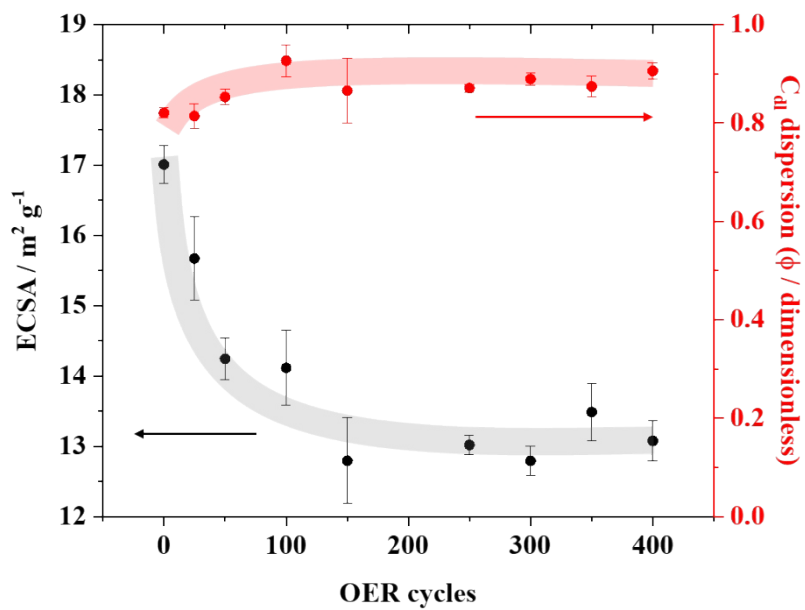


**Figure S5.** ECSA<sub>EIS</sub> and Cdl dispersion represented for Dy<sub>2</sub>NiRuO<sub>6</sub> OER cycles measured at 10 mV s<sup>-1</sup>.

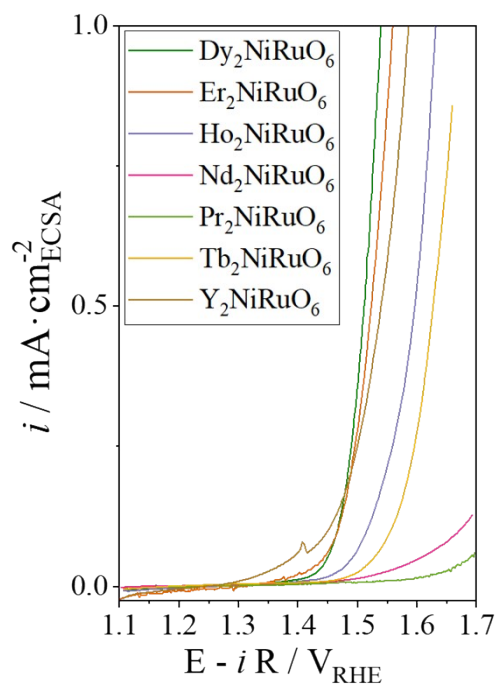


**Figure S6.** ECSA normalized activity of R<sub>2</sub>NiRuO<sub>6</sub> after 30 OER cycles.

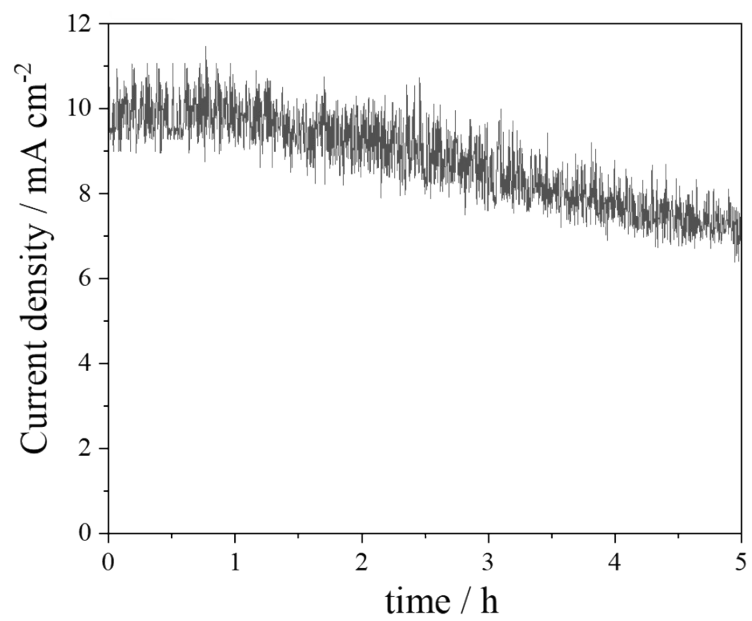


**Figure S7.** Chronoamperometry for Dy<sub>2</sub>NiRuO<sub>6</sub> at the potential where  $j \sim 10 \text{ mA cm}^{-2}$ , which is ca. 1.55 V.

### S3. TEM characterization

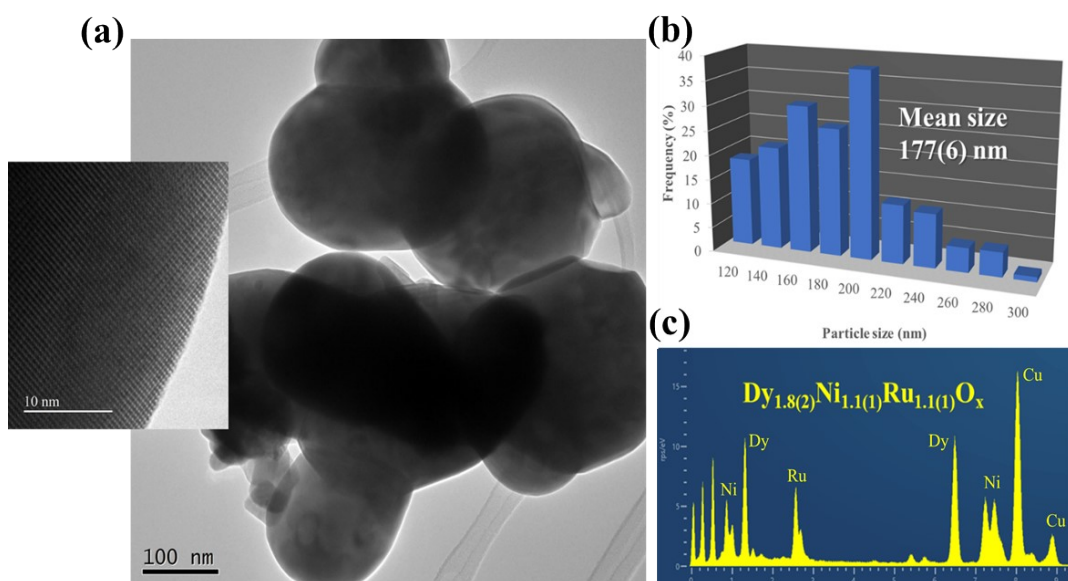


**Figure S8.** Initial  $Dy_2NiRuO_6$  catalyst. (a) TEM images of groups of particles. Inset: HRTEM. (b) Distribution and mean particle size. (c) EDX corroborating the stoichiometry obtained in the Rietveld analysis of XRD.

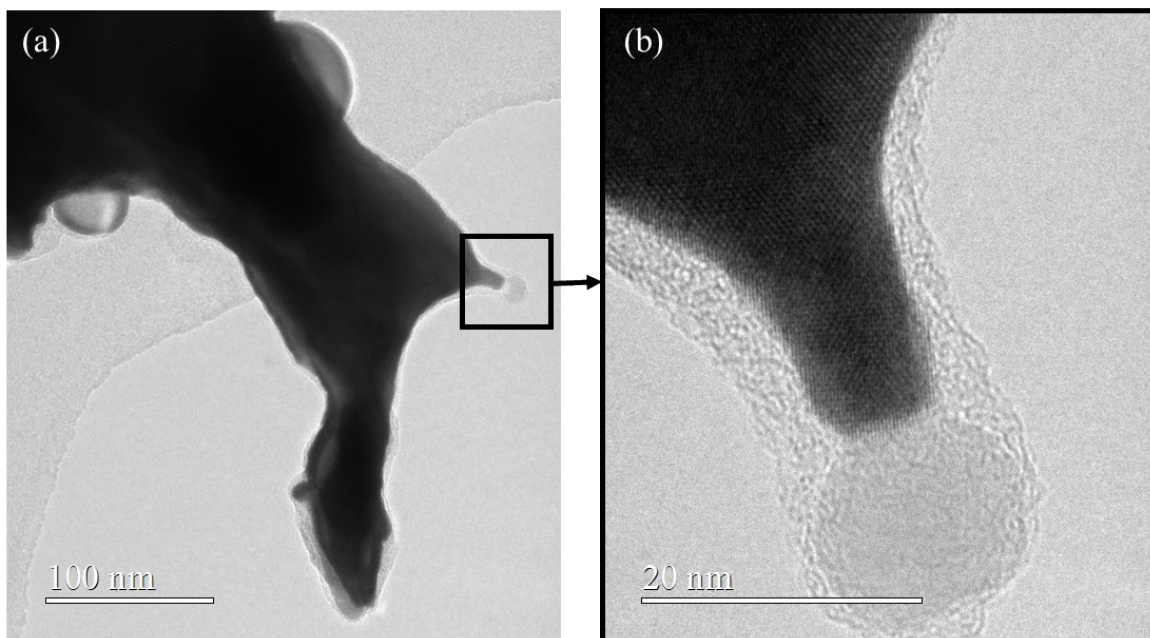


**Figure S9.** 100-cycles  $Dy_2NiRuO_6$  catalyst. (a) TEM image of a region of 100- $Dy_2NiRuO_6$  catalyst. (b) One of the isolated Ni-based particles formed during OER reaction.

#### S4. XPS results of the initial and cycled Dy<sub>2</sub>NiRuO<sub>6</sub> catalyst

Table S4. Surface atomic ratios.

	<i>Ru/Dy</i>	<i>Ru/Ni</i>	<i>Ni/Dy</i>
<b>Dy<sub>2</sub>NiRuO<sub>6</sub> Initial</b>	0.65	1.84	0.35
<b>Dy<sub>2</sub>NiRuO<sub>6</sub> 100 CV</b>	2.03	4.07	0.50
<b>Dy<sub>2</sub>NiRuO<sub>6</sub> 500 CV</b>	11.41	4.31	2.65
<b>Dy<sub>2</sub>NiRuO<sub>6</sub> 1000 CV</b>	8.33	2.54	3.28

## S5. Full computational details

The DFT calculations were made with the Vienna ab initio simulation package (VASP)<sup>23</sup> and making use of the PBE exchange-correlation functional<sup>24</sup> and the projector augmented-wave (PAW) method.<sup>25</sup> We used a plane-wave cutoff of 400 eV for the plane-wave basis set and the atoms were relaxed until the residual forces were less than 0.05 eV Å<sup>-1</sup>. All calculations were spin unrestricted. To enable a cost-effective localization of the electrons, we used Dudarev et al's GGA+U approach,<sup>26</sup> with  $U_{\text{eff}} = 6.70$  eV on the Ru ions, found by Xu et al. for Ru<sup>4+</sup> by means of a linear-response method;<sup>27</sup> and  $U_{\text{eff}} = 6.01$  eV on the Ni ions, which is the average of the values found by Zhou et al. for Ni<sup>2+</sup>, Ni<sup>3+</sup> and Ni<sup>4+</sup>.<sup>28</sup> The k-points for the pristine and dissolved perovskites used to model the OER were chosen as Monkhorst-Pack grids<sup>29</sup> with a sampling of 4×4×1. The Methfessel-Paxton method<sup>29,30</sup> was used to smear the Fermi level with  $k_{\text{B}}T = 0.01$  eV and the energies were extrapolated to 0 K. To avoid spurious electrostatic interactions, a vacuum layer of more than 16 Å separated the periodically repeated images of the slabs, and dipole corrections were also applied in the vertical direction. H<sub>2</sub> and H<sub>2</sub>O were calculated in boxes of 15×15×15 Å<sup>3</sup>, sampling the  $\Gamma$ -point only and with Gaussian smearing and  $k_{\text{B}}T = 0.001$  eV.

The adsorption free energies of \*O, \*OH and \*OOH were evaluated as (see Table S5):  $\Delta G_{\text{ads}} \approx \Delta E_{\text{ads}} + \Delta ZPE - T\Delta S$ , where  $\Delta E_{\text{ads}}$  is the DFT-calculated binding energy,  $\Delta ZPE$  is the zero-point energy change calculated with DFT using the harmonic oscillator approximation (the ZPEs of \*O, \*OH and \*OOH are 0.07, 0.36 and 0.43 eV, those of H<sub>2</sub> and H<sub>2</sub>O are 0.28 and 0.58 eV), and  $T\Delta S$  are entropy corrections, which include all sorts of contributions for H<sub>2</sub> and H<sub>2</sub>O (0.40 and 0.67 eV for H<sub>2</sub> and H<sub>2</sub>O). The computational hydrogen electrode approach<sup>31</sup> was used to evaluate the energetics of protons and electrons.<sup>31</sup> Water-adsorbate interactions were incorporated in the shape of ad hoc corrections taken from the literature,<sup>32</sup> for \*O, \*OH and \*OOH on Ni/Ru sites:  $-0.26 \pm 0.16/-0.40 \pm 0.10$ ,  $-0.46 \pm 0.10/-0.32 \pm 0.08$ ,  $-0.33 \pm 0.11/-0.34 \text{ eV} \pm 0.08$ . These values are averages and the error bars correspond to the standard deviation of the data. Water solvation for adsorbates on Ru sites is assumed to be similar to that of Fe.

To simulate the structures upon Dy dissolution, we first removed the Dy ions from the slabs and relaxed again the structures. To simulate the loss of Ni, we first replaced Ni ions at the top layer by Ru ions (referred to as “less Ni” in Figure 6), and then replaced



all of the Ni ions by Ru ions (referred to as “no Ni” in Figure 6). The most active surface of Dy<sub>2</sub>NiRuO<sub>6</sub> upon Dy dissolution is shown in Figure S10. Converged coordinates of all slabs appear at the end of this section.

The OER was assumed to proceed as:<sup>1,5,33,34</sup>



The free energies of those equations are, respectively:  $\Delta G_1 = \Delta G_{OH}$ ,  $\Delta G_2 = \Delta G_O - \Delta G_{OH}$ ,  $\Delta G_3 = \Delta G_{OOH} - \Delta G_O$  and  $\Delta G_4 = \Delta G_{O_2} - \Delta G_{OOH}$ .  $\Delta G_{OH}$ ,  $\Delta G_O$  and  $\Delta G_{OOH}$  are defined using protons, electrons, and water as references. The OER overpotential was calculated as:  $\eta_{OER} = \max(\Delta G_1, \Delta G_2, \Delta G_3, \Delta G_4)/e^- - 1.23$ . As shown previously,<sup>1,5</sup> experimental OER data may be added to computational activity plots using Seh *et al*'s<sup>33</sup> semiempirical volcano. The electrochemical-step symmetry index (ESSI) quantifies electrocatalytic

symmetry and is defined as (see Table S5):  $ESSI = \sum_{i=1}^n (\Delta G_i^+ / e^- - U^0) / n$ , where  $\Delta G_i^+$  are the free energies of the electrochemical steps larger than 1.23 eV.<sup>35-37</sup> The thermodynamically ideal catalyst has  $n = 4$ ,  $\Delta G_i^+ = 1.23$  eV, and  $ESSI = 0$ . Real catalysts have  $n$  between 1 and 3 and highly active OER electrocatalysts are often display  $n = 3$ .<sup>37</sup>

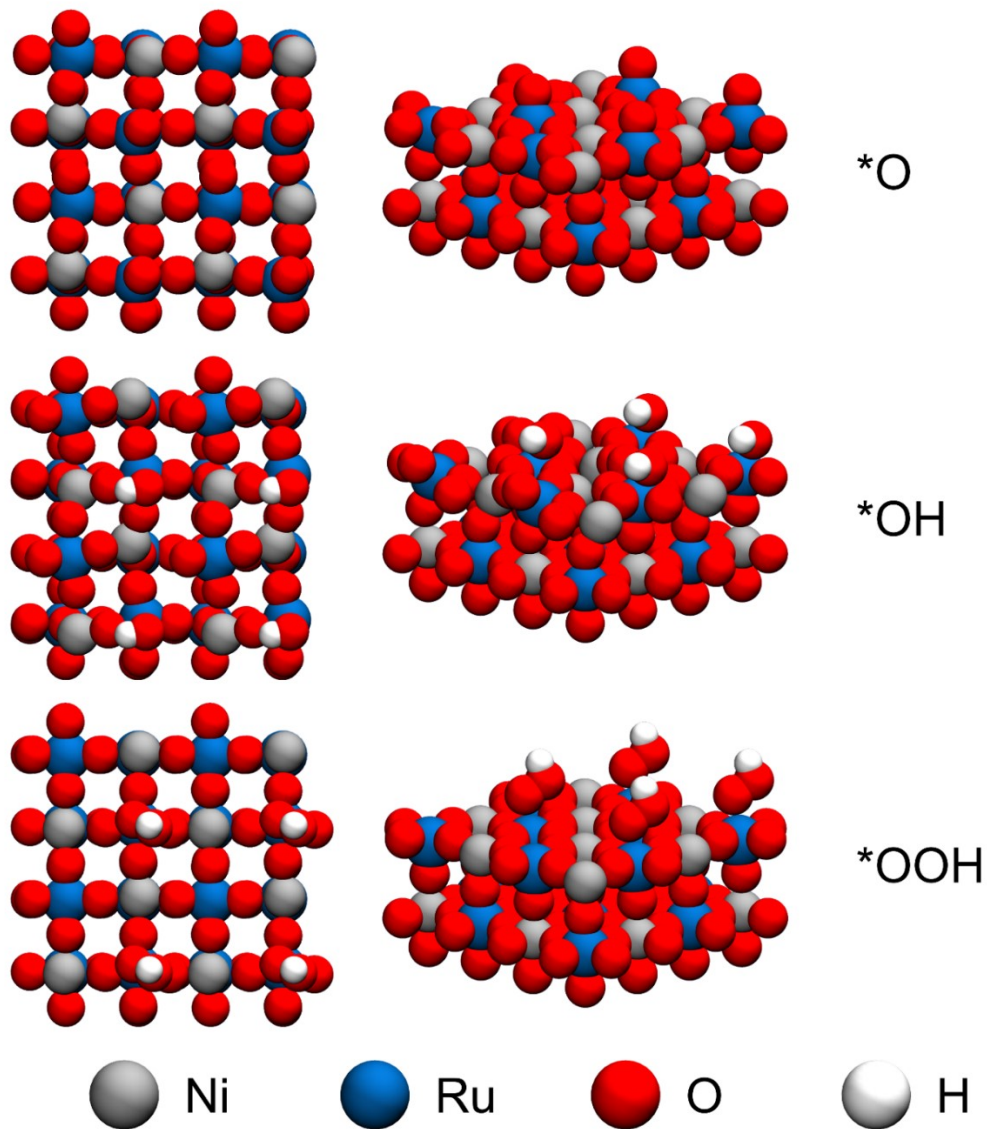


**Figure S10.** Schematics of NiRuO<sub>x</sub> overlayers on Dy<sub>2</sub>NiRuO<sub>6</sub> with OER adsorbates on Ru sites. Left: top views. Right: lateral views.

**Table S5.** Adsorption energies (eV), ESSI (V), OER overpotential (V), and potential-limiting step (abbreviated as PLS) for various sites on pristine and defective Dy<sub>2</sub>NiRuO<sub>6</sub>.

system	site	$\Delta G_O$	$\Delta G_{OH}$	$\Delta G_{OOH}$	ESSI	$\eta_{OER}$	PLS
pristine	Ni	3.97	1.50	4.55	0.76	1.24	2
	Ru	2.05	0.44	3.68	0.26	0.40	3
Dy dissolved	Ni	2.75	0.16	2.52	1.26	1.36	2
	Ru	2.70	1.12	3.55	0.24	0.34	2
less Ni	Ru	1.55	0.44	3.82	1.04	1.04	3
no Ni	Ru	1.19	0.76	3.63	0.64	1.22	3
1% strain	Ru	2.93	1.20	4.21	0.28	0.50	2
2% strain	Ru	3.32	1.34	4.20	0.43	0.75	2



0.236200882990875 0.2880178003868754 0.2251571060780266 T T T
0.7785180012136576 0.7250467393818910 0.2254512921806080 T T T
0.2500000000000000 0.2500000000000000 0.0775086000000016 F F F
0.7500000000000000 0.7500000000000000 0.0775086000000016 F F F
0.2785368834810113 0.731984042069457 0.2289384481931239 T T T
0.7117039170327002 0.2106048851093764 0.2467545262955736 T T T
0.2500000000000000 0.2500000000000000 0.0000000000000000 F F F
0.0000000000000000 0.2500000000000000 0.0775086000000016 F F F
0.2500000000000000 0.0000000000000000 0.0775086000000016 F F F
0.2500000000000000 0.7500000000000000 0.0000000000000000 F F F
0.2500000000000000 0.7500000000000000 0.0000000000000000 F F F
0.2500000000000000 0.5000000000000000 0.0775086000000016 F F F
0.7500000000000000 0.2500000000000000 0.0000000000000000 F F F
0.5000000000000000 0.2500000000000000 0.0775086000000016 F F F
0.7500000000000000 0.0000000000000000 0.0775086000000016 F F F
0.7500000000000000 0.7500000000000000 0.0000000000000000 F F F
0.5000000000000000 0.7500000000000000 0.0775086000000016 F F F
0.7500000000000000 0.0000000000000000 0.0775086000000016 F F F
0.5000000000000000 0.7500000000000000 0.0000000000000000 F F F
0.7500000000000000 0.0000000000000000 0.0775086000000016 F F F
0.2500000000000000 0.2499472624172503 0.1510795876890785 T T T
0.0164827008931361 0.25019429723438870 0.2358446478261557 T T T
0.2625308042736657 0.9205081738744539 0.263928493937032 T T T
0.226650294945708 0.758115784995475 0.1628248512333789 T T T
0.0019015296316762 0.7362408018750777 0.2501828985116976 T T T
0.2330656012859142 0.5224810299985717 0.2547523272519306 T T T
0.781114539190573 0.2716121081515687 0.1751509364149069 T T T
0.4823369870970334 0.2344818740417075 0.2387210490503580 T T T
0.7260265613263498 0.016378505160219 0.2383447761341066 T T T
0.7573170003300771 0.7499583941386746 0.150263832673864 T T T
0.502695310915029 0.7108117442613726 0.22469582862398 T T T
0.763981943491188 0.471863226433515 0.2350302847372383 T T T
0.7464718069963274 0.2483090348495669 0.312691465423696 T T T
By-dissolved with \*OH @ Ru:
1.0000000000000000
7.7508600000000003 0.0000000000000000 0.0000000000000000
0.0000000000000000 7.7508600000000003 0.0000000000000000
0.0000000000000000 0.0000000000000000 25.0000000000000000
Ni Ru O H
4 4 2 5 1
Selective dynamics
Direct
0.2500000000000000 0.7500000000000000 0.0775086000000016 F F F
0.7500000000000000 0.2500000000000000 0.0775086000000016 F F F
0.3332658845113549 0.1854083690270979 0.2175536245021642 T T T
0.6964545823700974 0.8173981346606498 0.2180099143600128 T T T
0.2500000000000000 0.2500000000000000 0.0775086000000016 F F F
0.7500000000000000 0.7500000000000000 0.0775086000000016 F F F
0.2739227811228253 0.708656859417219 0.2289473466045806 T T T
0.7821943778561877 0.286264823354943 0.2299390392184534 T T T
0.2500000000000000 0.2500000000000000 0.0000000000000000 F F F
0.0000000000000000 0.2500000000000000 0.0775086000000016 F F F
0.2500000000000000 0.0000000000000000 0.0775086000000016 F F F
0.2500000000000000 0.7500000000000000 0.0000000000000000 F F F
0.0000000000000000 0.7500000000000000 0.0775086000000016 F F F
0.2500000000000000 0.5000000000000000 0.0775086000000016 F F F
0.7500000000000000 0.2500000000000000 0.0000000000000000 F F F
0.2500000000000000 0.2500000000000000 0.0000000000000000 F F F
0.2500000000000000 0.7500000000000000 0.0000000000000000 F F F
0.7500000000000000 0.0000000000000000 0.0775086000000016 F F F
0.7500000000000000 0.5000000000000000 0.0775086000000016 F F F
0.255220816464228 0.2508044391330552 0.1539819897373324 T T T
0.0021807547020191 0.2695018589320823 0.2340085178589533 T T T
0.2731529281086337 0.9820441788552379 0.2455434646421120 T T T
0.2252640250172112 0.757957207128788 0.164009268626802 T T T
0.09731811724514 0.7107783178490499 0.2685904751426800 T T T
0.323379516981134 0.4925035395887546 0.225928857069510 T T T
0.743978697408573 0.2638231642552932 0.1622018802876548 T T T
0.5460021363213030 0.2184409592757360 0.249990134855077 T T T
0.7663238112548857 0.0193498409137919 0.2419346094877476 T T T
0.7485752139384437 0.737158457489925 0.156395047018647 T T T
0.480558254093706 0.775660951768612 0.2534910833064488 T T T
0.7426054980818299 0.4984471704504753 0.244267055138998 T T T
0.8042693050172589 0.202394459913936 0.3092020080893195 T T T
0.681751628053061 0.1816570900220143 0.3179729661861633 T T T
By-dissolved with \*OOH @ Ru:
1.0000000000000000
7.7508600000000003 0.0000000000000000 0.0000000000000000
0.0000000000000000 7.7508600000000003 0.0000000000000000
0.0000000000000000 0.0000000000000000 25.0000000000000000
Ni Ru O H
4 4 2 6 1
Selective dynamics
Direct
0.2500000000000000 0.7500000000000000 0.0775086000000016 F F F
0.7500000000000000 0.2500000000000000 0.0775086000000016 F F F
0.2365086212090220 0.2367405615827241 0.2305518387705541 T T T
0.7606224635288070 0.766195004110543 0.2300530826521222 T T T
0.2500000000000000 0.2500000000000000 0.0775086000000016 F F F
0.7500000000000000 0.7500000000000000 0.0775086000000016 F F F
0.2528066731580887 0.7401649242180046 0.226874826700774 T T T
0.743934492828721 0.2709725036840400 0.2291308793766607 T T T
0.2500000000000000 0.2500000000000000 0.0000000000000000 F F F
0.0000000000000000 0.2500000000000000 0.0775086000000016 F F F
0.0000000000000000 0.0000000000000000 0.0775086000000016 F F F
0.2500000000000000 0.7500000000000000 0.0000000000000000 F F F
0.0000000000000000 0.7500000000000000 0.0775086000000016 F F F
0.255040709912025 0.7127100675077847 0.2242656874937638 T T T
0.6909445213336692 0.1856018283062865 0.25530397757311 T T T
0.2500000000000000 0.2500000000000000 0.0000000000000000 F F F
0.0000000000000000 0.2500000000000000 0.0775086000000016 F F F
0.2500000000000000 0.0000000000000000 0.0775086000000016 F F F
0.0000000000000000 0.2500000000000000 0.0000000000000000 F F F
0.2500000000000000 0.0000000000000000 0.0775086000000016 F F F
0.0000000000000000 0.7500000000000000 0.0000000000000000 F F F
0.2500000000000000 0.7500000000000000 0.0000000000000000 F F F
0.2500000000000000 0.5000000000000000 0.0775086000000016 F F F
0.7500000000000000 0.2500000000000000 0.0000000000000000 F F F
0.7414089110453030 0.2441968803190551 0.242949782639517 T T T
0.482045158963034 0.237165032301965 0.247768500436800 T T T
0.737125230969758 0.015220364980154 0.2487302499130605 T T T
0.7327372281117653 0.7587535434903178 0.1599306911095312 T T T
0.4995865022621780 0.7421684807627120 0.249237759492022 T T T
0.7320870311548829 0.506839734872149 0.2445567786614299 T T T
0.72020907807483 0.2802513813134166 0.3229393824492329 T T T
0.8532044458426791 0.2188393424686125 0.3528003370118052 T T T
0.820717571018365 0.2545341657426712 0.3894934523146847 T T T
No Ni clean:
1.0000000000000000
7.7508600000000003 0.0000000000000000 0.0000000000000000
0.0000000000000000 7.7508600000000003 0.0000000000000000
0.0000000000000000 0.0000000000000000 25.0000000000000000
Ru O
0.7501686162571224 0.7315467136690222 0.159808389554589 T T T
0.7500000000000000 0.0000000000000000 0.0775086000000016 F F F
0.7500000000000000 0.0000000000000000 0.0000000000000000 F F F
0.5000000000000000 0.7500000000000000 0.0775086000000016 F F F
0.0226000516866327 0.7509057888457034 0.2491414456634470 T T T
0.2458012926782436 0.507839948546378 0.2436973610176739 T T T
0.7485689042172956 0.2524067238204327 0.1608351210672340 T T T
0.5215752568517887 0.2417063001889546 0.2434972540793935 T T T
0.7486703324883508 0.0142750323786205 0.2479374049590252 T T T
0.7501178550347762 0.7509487396013578 0.1539058066407594 T T T
0.4791013965742137 0.7487056530918387 0.2473349960326810 T T T
0.7515308366784784 0.4977815139596694 0.237901085431243 T T T
0.7192729148413785 0.2998359239816681 0.3297381010235765 T T T
0.856276958217084 0.2411818203739296 0.357141283698250 T T T
0.8244199362961804 0.2604219485260556 0.3951053879520234 T T T
Less Ni clean:
1.0000000000000000
7.7508600000000003 0.0000000000000000 0.0000000000000000
0.0000000000000000 7.7508600000000003 0.0000000000000000
0.0000000000000000 0.0000000000000000 25.0000000000000000
Ni Ru O
2 6 2 4
Selective dynamics
Direct
0.2500000000000000 0.7500000000000000 0.0775086000000016 F F F
0.7500000000000000 0.2500000000000000 0.0775086000000016 F F F
0.2500000000000000 0.2500000000000000 0.2308368143171349 T T T
0.7500000000000000 0.7500000000000000 0.2308368143171349 T T T
0.2500000000000000 0.2500000000000000 0.0775086000000016 F F F
0.7500000000000000 0.7500000000000000 0.0775086000000016 F F F
0.2500000000000000 0.2500000000000000 0.2308821176112478 T T T
0.7500000000000000 0.2500000000000000 0.2308821176112478 T T T
0.0000000000000000 0.2500000000000000 0.0000000000000000 F F F
0.2500000000000000 0.2500000000000000 0.0775086000000016 F F F
0.2500000000000000 0.0000000000000000 0.0775086000000016 F F F
0.2500000000000000 0.7500000000000000 0.0000000000000000 F F F
0.0000000000000000 0.7500000000000000 0.0775086000000016 F F F
0.0000000000000000 0.2500000000000000 0.0775086000000016 F F F
0.2500000000000000 0.2500000000000000 0.0000000000000000 F F F
0.2500000000000000 0.5000000000000000 0.0775086000000016 F F F
0.7500000000000000 0.2500000000000000 0.2308821176112478 T T T
0.7500000000000000 0.2500000000000000 0.2308821176112478 T T T
0.0006723454707970 0.2500000000000000 0.2459173011889324 T T T
0.2500000000000000 0.0006723454707970 0.2459173011889324 T T T
0.2500000000000000 0.2500000000000000 0.160544257475392 T T T
-0.0006723454707970 0.7500000000000000 0.2459173011889324 T T T
0.2500000000000000 0.4993276545929209 0.2459173011889324 T T T
0.7500000000000000 0.2500000000000000 0.160544257475392 T T T
0.4993276545929209 0.2500000000000000 0.2459173011889324 T T T
0.7500000000000000 -0.0006723454707970 0.2459173011889324 T T T
0.7500000000000000 0.7500000000000000 0.1594207312242809 T T T
0.5006723454707971 0.7500000000000000 0.2459173011889324 T T T
0.7500000000000000 0.5006723454707970 0.2459173011889324 T T T
Less Ni with \*O @ Ru:
1.0000000000000000
7.7508600000000003 0.0000000000000000 0.0000000000000000
0.0000000000000000 7.7508600000000003 0.0000000000000000
0.0000000000000000 0.0000000000000000 25.0000000000000000
Ni Ru O H
2 6 2 5
Selective dynamics
Direct
0.2500000000000000 0.7500000000000000 0.0775086000000016 F F F
0.7500000000000000 0.2500000000000000 0.0775086000000016 F F F
0.2555040709912025 0.7127100675077847 0.2242656874937638 T T T
0.6909445213336692 0.1856018283062865 0.25530397757311 T T T
0.2500000000000000 0.2500000000000000 0.0000000000000000 F F F
0.0000000000000000 0.2500000000000000 0.0775086000000016 F F F
0.2500000000000000 0.0000000000000000 0.0775086000000016 F F F
0.0000000000000000 0.2500000000000000 0.0000000000000000 F F F
0.2500000000000000 0.0000000000000000 0.0775086000000016 F F F
0.0000000000000000 0.7500000000000000 0.0000000000000000 F F F
0.2500000000000000 0.7500000000000000 0.0000000000000000 F F F
0.255040709912025 0.7127100675077847 0.2242656874937638 T T T
0.6909445213336692 0.1856018283062865 0.25530397757311 T T T
0.2500000000000000 0.2500000000000000 0.0000000000000000 F F F
0.0000000000000000 0.2500000000000000 0.0775086000000016 F F F
0.2500000000000000 0.0000000000000000 0.0775086000000016 F F F
0.0000000000000000 0.2500000000000000 0.0000000000000000 F F F
0.2500000000000000 0.0000000000000000 0.0775086000000016 F F F
0.0000000000000000 0.7500000000000000 0.0000000000000000 F F F
0.2500000000000000 0.7500000000000000 0.0000000000000000 F F F
0.255040709912025 0.7127100675077847 0.2242656874937638 T T T
0.6909445213336692 0.1856018283062865 0.25530397757311 T T T
0.2500000000000000 0.2500000000000000 0.0000000000000000 F F F
0.0000000000000000 0.2500000000000000 0.0775086000000016 F F F
0.2500000000000000 0.0000000000000000 0.0775086000000016 F F F
0.0000000000000000 0.2500000000000000 0.0000000000000000 F F F
0.2500000000000000 0.0000000000000000 0.0775086000000016 F F F
0.0000000000000000 0.7500000000000000 0.0000000000000000 F F F
0.2500000000000000 0.7500000000000000 0.0000000000000000 F F F
0.255040709912025 0.7127100675077847 0.2242656874937638 T T T
0.6909445213336692 0.1856018283062865 0.25530397757311 T T T
0.2500000000000000 0.2500000000000000 0.0000000000000000 F F F
0.0000000000000000 0.2500000000000000 0.0775086000000016 F F F
0.2500000000000000 0.0000000000000000 0.0775086000000016 F F F
0.0000000000000000 0.2500000000000000 0.0000000000000000 F F F
0.2500000000000000 0.0000000000000000 0.0775086000000016 F F F
0.0000000000000000 0.7500000000000000 0.0000000000000000 F F F
0.2500000000000000 0.7500000000000000 0.0000000000000000 F F F
0.255040709912025 0.7127100675077847 0.2242656874937638 T T T
0.6909445213336692 0.1856018283062865 0.25530397757311 T T T
0.2500000000000000 0.2500000000000000 0.0000000000000000 F F F
0.0000000000000000 0.2500000000000000 0.0775086000000016 F F F
0.2500000000000000 0.0000000000000000 0.0775086000000016 F F F
0.0000000000000000 0.2500000000000000 0.0000000000000000 F F F
0.2500000000000000 0.0000000000000000 0.0775086000000016 F F F
0.0000000000000000 0.7500000000000000 0.0000000000000000 F F F
0.2500



```

7.8283686000000001 0.0000000000000000 0.0000000000000000
0.0000000000000000 7.8283686000000001 0.0000000000000000
0.0000000000000000 0.0000000000000000 25.0000000000000000
Ni Ru O H
4 4 26 1
Selective dynamics
Direct
0.2500000000000000 0.7500000000000000 0.0782836859999989 F F F
0.7500000000000000 0.2500000000000000 0.0782836859999989 F F F
0.4764745641267651 0.7500000000000000 0.2436174956846812 T T T
0.2480343054657649 0.2180635785034377 0.2272692832936443 T T T
0.7020803329936035 0.7593136940523173 0.224481676870714 T T T
0.2500000000000000 0.2500000000000000 0.0782836859999989 F F F
0.7500000000000000 0.7500000000000000 0.0782836859999989 F F F
0.2644660599426681 0.713573916031438 0.2330346817322296 T T T
0.7515753463611288 0.2586321400090963 0.2274927564292655 T T T
0.2500000000000000 0.2500000000000000 0.0000000000000000 F F F
0.0000000000000000 0.2500000000000000 0.0782836859999989 F F F
0.2500000000000000 0.0000000000000000 0.0782836859999989 F F F
0.2500000000000000 0.7500000000000000 0.0000000000000000 F F F
0.0000000000000000 0.7500000000000000 0.0782836859999989 F F F
0.2500000000000000 0.5000000000000000 0.0782836859999989 F F F
0.7500000000000000 0.2500000000000000 0.0000000000000000 F F F
0.5000000000000000 0.2500000000000000 0.0000000000000000 F F F
0.7500000000000000 0.0000000000000000 0.0782836859999989 F F F
0.7500000000000000 0.7500000000000000 0.0000000000000000 F F F
0.5000000000000000 0.7500000000000000 0.0782836859999989 F F F
0.2470038672590924 0.2488450988301978 0.1515776378654043 T T T
0.9821172610127462 0.2479267726522071 0.2403656459373938 T T T
0.261794494038933 -0.0004393330558827 0.2524948444305077 T T T
0.2394267540437207 0.7770982674679725 0.1683486591882917 T T T
0.088969076992439 0.7461814746056972 0.2718169788378201 T T T
0.265169554044278 0.4930243256147519 0.2288766617390032 T T T
0.7492187239804352 0.2553420270201545 0.159267389487918 T T T
0.5146405134460359 0.2401081277393290 0.2424463063969829 T T T
0.7333728255885859 0.0140257336891749 0.2413462575589404 T T T
0.7536230855423917 0.7505464178920845 0.1565070619397164 T T T
0.4697026587567464 0.7474029285186993 0.299358831869482 T T T
0.7395272879683851 0.4902730362318460 0.2412481413211271 T T T
0.736237283164698 0.2258283708549396 0.3218969169329384 T T T
0.8699347460057260 0.2928953509538313 0.3492115215710893 T T T
0.8488675239853560 0.2554275539240504 0.3864246719238120 T T T

% strain clean:
1.0000000000000000
7.9058771999999999 0.0000000000000000 0.0000000000000000
0.0000000000000000 7.9058771999999999 0.0000000000000000
0.0000000000000000 0.0000000000000000 25.0000000000000000
Ni Ru O
4 4 24
Selective dynamics
Direct
0.2500000000000000 0.7500000000000000 0.0790587720000033 F F F
0.7500000000000000 0.2500000000000000 0.0790587720000033 F F F
0.2500000000000000 0.2500000000000000 0.2310047350213059 T T T
0.7500000000000000 0.7500000000000000 0.2310047350213059 T T T
0.2500000000000000 0.2500000000000000 0.0790587720000033 F F F
0.7500000000000000 0.7500000000000000 0.0790587720000033 F F F
0.2500000000000000 0.7500000000000000 0.2287490038265501 T T T
0.7500000000000000 0.2500000000000000 0.2287490038265501 T T T
0.2500000000000000 0.2500000000000000 0.0000000000000000 F F F
0.0000000000000000 0.2500000000000000 0.0790587720000033 F F F
0.2500000000000000 0.0000000000000000 0.0790587720000033 F F F
0.2500000000000000 0.7500000000000000 0.0000000000000000 F F F
0.0000000000000000 0.7500000000000000 0.0000000000000000 F F F
0.5000000000000000 0.7500000000000000 0.0790587720000033 F F F
0.7500000000000000 0.2500000000000000 0.0000000000000000 F F F
0.2500000000000000 0.2500000000000000 0.0790587720000033 F F F
0.7500000000000000 0.0000000000000000 0.0790587720000033 F F F
0.2492013629075115 0.749566829557253 0.2333979794353505 T T T
0.7294844135788060 0.1861047205353400 0.2307791269406888 T T T
0.2500000000000000 0.2500000000000000 0.0000000000000000 F F F
0.2500000000000000 0.2500000000000000 0.0790587720000033 F F F
0.9764745641267651 0.2500000000000000 0.2436174956846812 T T T
0.2500000000000000 0.9764745641267651 0.2436174956846812 T T T
0.2500000000000000 0.7500000000000000 0.0000000000000000 F F F
0.0000000000000000 0.7500000000000000 0.1603605107143168 T T T
0.0235254358732349 0.7500000000000000 0.2436174956846812 T T T
0.2500000000000000 0.2500000000000000 0.2436174956846812 T T T
0.7500000000000000 0.2500000000000000 0.1603605107143168 T T T
0.5235254358732349 0.2500000000000000 0.2436174956846812 T T T
0.7500000000000000 0.2500000000000000 0.0790587720000033 F F F
0.7500000000000000 0.2500000000000000 0.0000000000000000 F F F
0.7500000000000000 0.7500000000000000 0.1548038780301353 T T T
0.4764745641267651 0.7500000000000000 0.2436174956846812 T T T
0.7500000000000000 0.4764745641267651 0.2436174956846812 T T T
1.0000000000000000
7.9058771999999999 0.0000000000000000 0.0000000000000000
0.0000000000000000 7.9058771999999999 0.0000000000000000
0.0000000000000000 0.0000000000000000 25.0000000000000000
Ni Ru O
4 4 25
Selective dynamics
Direct
0.2500000000000000 0.7500000000000000 0.0790587720000033 F F F
0.7500000000000000 0.2500000000000000 0.0790587720000033 F F F
0.3383543171008964 0.1860995959459372 0.217878252130656 T T T
0.7515392771810354 0.8113086185914337 0.2233964130322469 T T T
0.2500000000000000 0.2500000000000000 0.0790587720000033 F F F
0.7500000000000000 0.7500000000000000 0.0790587720000033 F F F
0.228382403388083 0.7752083955366573 0.2347816757066021 T T T
0.8121836308719879 0.2993630664615811 0.2498096835827617 T T T
0.2500000000000000 0.2500000000000000 0.0000000000000000 F F F
0.0000000000000000 0.2500000000000000 0.0790587720000033 F F F
0.0000000000000000 0.2500000000000000 0.0000000000000000 F F F
0.0000000000000000 0.2500000000000000 0.0790587720000033 F F F
0.2500000000000000 0.0000000000000000 0.0790587720000033 F F F
0.2500000000000000 0.7500000000000000 0.0000000000000000 F F F
0.0000000000000000 0.7500000000000000 0.0790587720000033 F F F
0.2500000000000000 0.5000000000000000 0.0790587720000033 F F F
0.7500000000000000 0.2500000000000000 0.0000000000000000 F F F
0.5000000000000000 0.2500000000000000 0.0000000000000000 F F F
0.7500000000000000 0.0000000000000000 0.0790587720000033 F F F
0.2470038672590924 0.2488450988301978 0.1515776378654043 T T T
0.9821172610127462 0.2479267726522071 0.2403656459373938 T T T
0.261794494038933 -0.0004393330558827 0.2524948444305077 T T T
0.2394267540437207 0.7770982674679725 0.1683486591882917 T T T
0.088969076992439 0.7461814746056972 0.2718169788378201 T T T
0.265169554044278 0.4930243256147519 0.2288766617390032 T T T
0.7492187239804352 0.2553420270201545 0.159267389487918 T T T
0.5146405134460359 0.2401081277393290 0.2424463063969829 T T T
0.7333728255885859 0.0140257336891749 0.2413462575589404 T T T
0.7536230855423917 0.7505464178920845 0.1565070619397164 T T T
0.4697026587567464 0.7474029285186993 0.299358831869482 T T T
0.7395272879683851 0.4902730362318460 0.2412481413211271 T T T
0.736237283164698 0.2258283708549396 0.3218969169329384 T T T
0.8699347460057260 0.2928953509538313 0.3492115215710893 T T T
0.8488675239853560 0.2554275539240504 0.3864246719238120 T T T

% strain with *OH:
1.0000000000000000
7.9058771999999999 0.0000000000000000 0.0000000000000000
0.0000000000000000 7.9058771999999999 0.0000000000000000
0.0000000000000000 0.0000000000000000 25.0000000000000000
Ni Ru O H
4 4 26 1
Selective dynamics
Direct
0.2500000000000000 0.7500000000000000 0.0790587720000033 F F F
0.7500000000000000 0.2500000000000000 0.0790587720000033 F F F
0.3567022074621277 0.1811737861821296 0.2177681121279409 T T T
0.8073515885069831 0.867991466823656 0.209194380891891 T T T
0.2500000000000000 0.2500000000000000 0.0790587720000033 F F F
0.7500000000000000 0.2500000000000000 0.0000000000000000 F F F
0.5000000000000000 0.7500000000000000 0.0790587720000033 F F F
0.3074556129746231 0.7559776038664621 0.2355671540213191 T T T
0.7723262597791192 0.282065863679538 0.2321315314926401 T T T
0.2500000000000000 0.2500000000000000 0.0000000000000000 F F F
0.0000000000000000 0.2500000000000000 0.0790587720000033 F F F
0.2500000000000000 0.0000000000000000 0.0790587720000033 F F F
0.2500000000000000 0.7500000000000000 0.0000000000000000 F F F
0.5000000000000000 0.7500000000000000 0.0790587720000033 F F F
0.0000000000000000 0.7500000000000000 0.0000000000000000 F F F
0.2500000000000000 0.5000000000000000 0.0790587720000033 F F F
0.7500000000000000 0.2500000000000000 0.0000000000000000 F F F
0.5000000000000000 0.2500000000000000 0.0000000000000000 F F F
0.7500000000000000 0.0000000000000000 0.0790587720000033 F F F
0.2489708557693816 0.2035344073301267 0.1564046853025922 T T T
0.9685247867795294 0.2038171729940419 0.2467541339866426 T T T
0.3056604783297795 0.968495721557728 0.2535543500070332 T T T
0.2432276986239520 0.7245244830463156 0.1714051983196149 T T T
0.9849630547919668 0.8569575148946111 0.2409058786856679 T T T
0.2046519882640997 0.6293791536758552 0.278972016619381 T T T
0.7739088429830968 0.3031506089946160 0.1640655053579541 T T T
0.5344321771223035 0.287006691096256 0.2455836175849934 T T T
0.6958439188734676 0.0383462447892247 0.2360541499315419 T T T
0.7397463789666215 0.7494217249856874 0.15799007850960553 T T T
0.5123296599735903 0.6983372933728227 0.2387197106388563 T T T
0.7871839767626545 0.4821107984723870 0.2575186134761555 T T T
0.7383677416739303 0.2218546387937063 0.331432046925282 T T T
0.8766077632119400 0.2691340453539759 0.3591701874041633 T T T
0.8515756362063858 0.234941826608998 0.3964882383915204 T T T

```

## S6. Additional references

- 1 M. Retuerto, L. Pascual, F. Calle-Vallejo, P. Ferrer, D. Gianolio, A. G. Pereira, Á. García, J. Torrero, M. T. Fernández-Díaz, P. Bencok, M. A. Peña, J. L. G. Fierro and S. Rojas, *Nat. Commun.*, 2019, **10**, 2041.
- 2 I. Rodríguez-García, D. Galyamin, L. Pascual, P. Ferrer, M. A. Peña, D. Grinter, G. Held, M. Abdel Salam, M. Mokhtar, K. Narasimharao, M. Retuerto and S. Rojas, *J. Power Sources*, 2022, **521**, 230950.
- 3 B.-J. Kim, D. F. Abbott, X. Cheng, E. Fabbri, M. Nachtegaal, F. Bozza, I. E. Castelli, D. Lebedev, R. Schäublin, C. Copéret, T. Graule, N. Marzari and T. J. Schmidt, *ACS Catal.*, 2017, **7**, 3245–3256.
- 4 X. Miao, L. Zhang, L. Wu, Z. Hu, L. Shi and S. Zhou, *Nat. Commun.*, 2019, **10**, 1–7.
- 5 D. Galyamin, J. Torrero, I. Rodríguez, M. J. Kolb, P. Ferrer, L. Pascual, M. A. Salam, D. Gianolio, V. Celorrio, M. Mokhtar, D. Garcia Sanchez, A. S. Gago, K. A. Friedrich, M. A. Peña, J. A. Alonso, F. Calle-Vallejo, M. Retuerto and S. Rojas, *Nat. Commun.*, 2023, **14**, 2010.
- 6 N. Zhang, C. Wang, J. Chen, C. Hu, J. Ma, X. Deng, B. Qiu, L. Cai, Y. Xiong and Y. Chai, *ACS Nano*, 2021, **15**, 8537–8548.
- 7 Q. Feng, Q. Wang, Z. Zhang, Y. Xiong, H. Li, Y. Yao, X. Z. Yuan, M. C. Williams, M. Gu, H. Chen, H. Li and H. Wang, *Appl. Catal. B Environ.*, 2019, **244**, 494–501.
- 8 J. Kim, P. Shih, Y. Qin, Z. Al-Bardan, C. Sun and H. Yang, *Angew. Chemie Int. Ed.*, 2018, **57**, 13877–13881.
- 9 D. A. Kuznetsov, M. A. Naeem, P. V. Kumar, P. M. Abdala, A. Fedorov and C. R. Müller, *J. Am. Chem. Soc.*, 2020, **142**, 7883–7888.
- 10 Q. Feng, J. Zou, Y. Wang, Z. Zhao, M. C. Williams, H. Li and H. Wang, *ACS Appl. Mater. Interfaces*, 2020, **12**, 4520–4530.
- 11 M. A. Hubert, A. M. Patel, A. Gallo, Y. Liu, E. Valle, M. Ben-Naim, J. Sanchez, D. Sokaras, R. Sinclair, J. K. Nørskov, L. A. King, M. Bajdich and T. F. Jaramillo, *ACS Catal.*, 2020, 12182–12196.
- 12 J. Kim, P. C. Shih, K. C. Tsao, Y. T. Pan, X. Yin, C. J. Sun and H. Yang, *J. Am. Chem. Soc.*, 2017, **139**, 12076–12083.
- 13 Y. Lin, Z. Tian, L. Zhang, J. Ma, Z. Jiang, B. J. Deibert, R. Ge and L. Chen, *Nat. Commun.*, , DOI:10.1038/s41467-018-08144-3.
- 14 S. Hao, M. Liu, J. Pan, X. Liu, X. Tan, N. Xu, Y. He, L. Lei and X. Zhang, *Nat. Commun.*, 2020, **11**, 5368.
- 15 C. Lin, J.-L. Li, X. Li, S. Yang, W. Luo, Y. Zhang, S.-H. Kim, D.-H. Kim, S. S. Shinde, Y.-F. Li, Z.-P. Liu, Z. Jiang and J.-H. Lee, *Nat. Catal.*, 2021, **4**, 1012–1023.
- 16 J. Su, R. Ge, K. Jiang, Y. Dong, F. Hao, Z. Tian, G. Chen and L. Chen, *Adv. Mater.*, 2018, **30**, 1–8.
- 17 J. Wang, Y. Ji, R. Yin, Y. Li, Q. Shao and X. Huang, *J. Mater. Chem. A*, 2019, **7**, 6411–6416.
- 18 Z. L. Zhao, Q. Wang, X. Huang, Q. Feng, S. Gu, Z. Zhang, H. Xu, L. Zeng, M. Gu and H. Li, *Energy Environ. Sci.*, 2020, **13**, 5143–5151.
- 19 Y. Yao, S. Hu, W. Chen, Z.-Q. Huang, W. Wei, T. Yao, R. Liu, K. Zang, X. Wang, G. Wu, W. Yuan, T. Yuan, B. Zhu, W. Liu, Z. Li, D. He, Z. Xue, Y. Wang, X. Zheng, J. Dong, C.-R. Chang, Y. Chen, X. Hong, J. Luo, S. Wei, W.-X. Li, P. Strasser, Y. Wu and Y. Li, *Nat. Catal.*, 2019, **2**, 304–313.
- 20 C. C. L. L. McCrory, S. Jung, J. C. Peters and T. F. Jaramillo, *J. Am. Chem. Soc.*, 2013, **135**, 16977–16987.
- 21 M. Retuerto, A. G. Pereira, F. Pérez-Alonso, M. A. Peña, J. L. G. Fierro, J. A. Alonso, M. T. Fernández-Díaz, L. Pascual and S. Rojas, *Appl. Catal. B Environ.*, 2017, **203**, 363–371.
- 22 A. Lasia, *J. Phys. Chem. Lett.*, 2022, **13**, 580–589.
- 23 G. Kresse and J. Furthmüller, *Phys. Rev. B - Condens. Matter Mater. Phys.*, 1996, **54**, 11169–11186.
- 24 J. P. Perdew, K. Burke and M. Ernzerhof, *Phys. Rev. Lett.*, 1996, **77**, 3865.
- 25 G. Kresse and D. Joubert, *Phys. Rev. B*, 1999, **59**, 1758–1775.
- 26 S. L. Dudarev, G. A. Botton, S. Y. Savrasov, C. J. Humphreys and A. P. Sutton, *Phys. Rev. B*, 1998, **57**, 1505–

- 1509.
- 27 Z. Xu, J. Rossmeisl and J. R. Kitchin, *J. Phys. Chem. C*, 2015, **119**, 4827–4833.
- 28 F. Zhou, M. Cococcioni, C. A. Marianetti, D. Morgan and G. Ceder, *Phys. Rev. B*, 2004, **70**, 235121.
- 29 H. J. Monkhorst and J. D. Pack, *Phys. Rev. B*, 1976, **13**, 5188–5192.
- 30 M. Methfessel and A. T. Paxton, *Phys. Rev. B*, 1989, **40**, 3616–3621.
- 31 J. K. Nørskov, J. Rossmeisl, A. Logadottir, L. Lindqvist, J. R. Kitchin, T. Bligaard and H. Jónsson, *J. Phys. Chem. B*, 2004, **108**, 17886–17892.
- 32 F. Calle-Vallejo, A. Krabbe and J. M. García-Lastra, *Chem. Sci.*, 2016, **8**, 124–130.
- 33 Z. W. Seh, J. Kibsgaard, C. F. Dickens, I. Chorkendorff, J. K. Nørskov and T. F. Jaramillo, *Science (80-. )*, 2017, **355**, eaad4998.
- 34 L. C. Seitz, C. F. Dickens, K. Nishio, Y. Hikita, J. Montoya, A. Doyle, C. Kirk, A. Vojvodic, H. Y. Hwang, J. K. Nørskov and T. F. Jaramillo, *Science (80-. )*, 2016, **353**, 1011–1014.
- 35 N. Govindarajan, J. M. García-Lastra, E. J. Meijer and F. Calle-Vallejo, *Curr. Opin. Electrochem.*, 2018, **8**, 110–117.
- 36 O. Piqué, F. Illas and F. Calle-Vallejo, *Phys. Chem. Chem. Phys.*, 2020, **22**, 6797–6803.
- 37 E. Romeo, F. Illas and F. Calle-Vallejo, *Chem. Sci.*, 2023, **14**, 3622–3629.